Research in Pharmaceutical Sciences, February 2026; 21(1): 77-95
Received: 11-07-2025
Peer Reviewed: 08-08-2025
Revised: 03-09-2025
Accepted: 22-09-2025
Published: 26-12-2025

School of Pharmacy & Pharmaceutical Sciences
Isfahan University of Medical Sciences

Original Article

Protective role of hydroalcoholic extract of *Medusomyces gisevii* L. in non-alcoholic fatty liver disease: insights from a murine model

Roozbeh Zare gashti[1], Mohammad Karami[2], Emran Habibi[3], Ali Abbasi[4], Shima Parsay[5], Mona Modanloo[6], Hasti Asadi Khalili[7], and Mohammad Shokrzadeh[6,*]

[1]*Department of Toxicology and Pharmacology, Faculty of Pharmacy, Mazandaran University of Medical Sciences, Sari, Iran*
[2]*Medicinal Plants Research Center, Institute of Herbal Medicines and Metabolic Disorders, Mazandaran University of Medical Sciences, Sari, Iran.*
[3]*Centre for Natural Products Discovery, School of Pharmacy and Biomolecular Sciences, Liverpool John Moores University, Liverpool L3 3AF, United Kingdom.*
[4]*Department of Pathology, Azad University, Sari Branch, Iran.*
[5]*Department of Medical Mycology, School of Medicine, Mazandaran University of Medical Sciences, Sari, Iran.*
[6]*Pharmaceutical Sciences Research Center, Hemoglobinopathy Institute, Mazandaran University of Medical Sciences, Sari, Iran.*
[7]*Department of Pharmacognosy and Biotechnology, Faculty of Pharmacy, Mazandaran University of Medical Sciences, Sari, Iran.*

Abstract

Background and purpose: This study explored the impact of the hydroalcoholic extract of *Medusomyces gisevii* L. (HEMG), a promising source for dietary use, on NAFLD in male mice.
Experimental approach: The essential oil of MG was characterized using GC-MS and the HEMG, obtained through continuous maceration. Male albino mice were subjected to 7 groups (n = 9), including normal diet, high-fat diet (HFD, 12 weeks), HEMG (62.5, 125, 250, and 500 mg/kg, orally, 8 weeks), or vitamin E (20 mg/kg, orally, 8 weeks) supplementation with HFD. Blood samples were analyzed for serum biomarkers, and liver mitochondria were isolated to assess oxidative stress markers. Histopathological examinations of liver tissue were conducted.
Findings/Results: MG was rich in cyclohexanol, carvacrol, and phenol, with HEMG exhibiting an antioxidant activity of 50.14 ± 3.56 µg/mL. It contained 73.47 ± 0.85 mg of gallic acid equivalents per g of TPC and 62.56 ± 1.30 mg/g of TTC, indicating the significant antioxidant properties of HEMG. Mice on an HFD exhibited elevated serum biomarkers, including ALT, AST, ALP, TG, TC, and LDL, along with a reduction in HDL levels. Oxidative stress factors, including ROS, protein carbonyl, and MDA, increased, while mitochondrial function, GSH, catalase, and SOD were decreased in the NAFLD groups. Furthermore, treatment with HEMG supplementation led to improvements in serum biomarkers and enhanced oxidative stress markers, thus alleviating liver damage and hepatic steatosis caused by the HFD.
Conclusion and implications: These results suggest that HEMG holds promise as a candidate in addressing NAFLD.

Keywords: Kombucha; Liver enzymes; *Medusomyces gisevii*; Non-alcoholic fatty liver disease; Oxidative stress; Vitamin E.

INTRODUCTION

The liver, recognized as the central site for lipid metabolism, plays a crucial role in processing fatty acids derived from food into energy necessary for the function of hepatocytes. However, when the liver accumulates triglycerides (TG) beyond 5% of its weight, it encounters functional challenges, resulting in the onset of fatty liver disease (1).

Access this article online	
	Website: http://rps.mui.ac.ir
	DOI: 10.4103/RPS.RPS_121_25

*Corresponding author: M. Shokrzadeh
Tel: +98-9111263448, Fax: +98-1133543084
Email: mshokrzadeh@mazums.ac.ir

Non-alcoholic fatty liver (NAFL) is defined as all cases characterized by steatosis, with or without mild lobular inflammation (2). NAFLD has evolved from being a relatively obscure condition to becoming the most prevalent cause of chronic liver disease worldwide (3) and exhibits strong associations with prevalent metabolic conditions like type 2 diabetes, obesity, hyperlipidemia, and hypertension (4), excluding excessive alcohol consumption and other chronic liver diseases (5). The progression of non-alcoholic fatty liver disease (NAFLD) can evolve from NAFL to more severe stages, including non-alcoholic steatohepatitis (NASH), cirrhosis, liver cancer, and ultimately, advanced liver disease and failure (6).

When the intake of energy surpasses its usage, the surplus energy is accumulated as lipids. In a disordered physiological state, lipids are deposited in various organs across the body (7). NAFLD serves as a classic example of the abnormal accumulation of lipids in non-adipose tissues. The development of hepatic steatosis in NAFLD results from an overproduction of TG in liver cells, with 60% of the materials for this production coming from white adipose tissue, 26% from *de novo* lipogenesis, and 15% from a diet high in fats and/or sugars (8).

Oxidative stress plays a crucial role in NAFLD, contributing significantly to both intrahepatic and extrahepatic complications. This imbalance in oxidative processes arises from an abundance of reactive oxygen species (ROS), like superoxide or hydrogen peroxide, combined with weakened antioxidant defenses. Factors such as high levels of free fatty acids and excess lipids in the liver worsen this condition, leading to an increase in ROS and compromised antioxidant mechanisms. These oxidative stress processes, linked to issues in cell parts like mitochondria and the endoplasmic reticulum, not only affect the liver's structure and function but also harm other parts of the body, like muscles, the heart, kidneys, and the nervous system (9,10).

The search for effective treatments for NAFLD continues, largely due to the complex nature of how the disease progresses and the incomplete understanding of its mechanisms (11). Current approaches recommended by the FDA focus on weight loss and physical activity, with at least a 10% reduction in body weight considered essential for histological improvements. While medications like silymarin, pioglitazone, and vitamin E have been employed in NAFLD treatment, their efficacy in definitively treating the disease remains inconclusive (12-14). However, ongoing research and clinical trials offer hope for identifying definitive therapeutic interventions for NAFLD and NASH, suggesting potential advancements in this domain (15).

In this context, it is crucial to explore innovative methods to address NAFLD, with one promising approach involving the use of plant-based substances and their derivatives, a subject of numerous scientific investigations (16-19). Of specific interest is *Medusomyces gisevii* L. (MG), a natural symbiont well-known for its potential as a dietary source, commonly known as Kombucha or Tea Fungus (20). MG is composed of a diverse microbial community, including yeasts and acetic acid bacteria. During the cultivation of symbionts, the culture medium accumulates different components. This includes residual nutrient substrates as well as byproducts resulting from microbial activity, which diffuse throughout the medium. It presents a range of health benefits associated with its rich composition of organic acids, vitamins, polyphenols, and potent antioxidants (21,22). The fermentation process of Kombucha also produces compounds with strong antioxidant properties, effectively scavenging free radicals and ROS (23). Previous research has highlighted the protective effects of Kombucha tea on different organs, demonstrating its ability to improve liver function indicators in damaged livers (24).

Despite the extensive existing research, there is a lack of sufficient evidence regarding the therapeutic potential of the hydroalcoholic extract of *Medusomyces gisevii* L. (HEMG) for treating NAFLD. Therefore, there is a compelling need to design an animal model study to investigate the therapeutic effects of HEMG on NAFLD, thereby uncovering a potentially novel therapeutic approach for this widespread liver disorder.

MATERIALS AND METHODS

Chemicals and reagents

Vitamin E, ketamine hydrochloride, xylazine hydrochloride, 3-[4, 5-dimethylthiazol-2-yl]-2, 5-diphenyltetrazolium bromide (MTT), 2, 7-dichlorodihydrofluorescein diacetate (DCFH-DA), 2, 4-dinitrophenylhydrazine (DNPH), thiobarbituric acid (TBA), trichloroacetic acid (TCA) and 5, 5-dithiobis[2-nitrobenzoic acid] (DTNB) used in this study were provided from Sigma Chemical Co. (St. Louis, MO, USA). Mannitol, sucrose, monopotassium phosphate (KH_2PO_4), ethylenediaminetetraacetic acid (EDTA), phosphoric acid, disodium hydrogen phosphate (Na_2HPO_4), methanol, HCl, Folin-Ciocâlteu, gallic acid, sodium carbonate, potassium acetate, sodium acetate, dimethyl sulfoxide (DMSO), and n-butanol used in this study were provided by Merck (Darmstadt, Germany). Superoxide dismutase (SOD) detection kits were obtained from ZellBio GmbH, Germany (Catalog number: ZX-44108). Alanine transaminase (ALT), aspartate aminotransferase (AST), alkaline phosphatase (ALP), total cholesterol (TC), TG, high-density lipoprotein (HDL), and low-density lipoproteins (LDL) kits were purchased from Pars Azmoon, Tehran, Iran. All other chemicals and solvents were of the highest available grade.

Preparation of MG extract

The MG samples (Fig. S1) were obtained from the Vandchali Center in Qaem Shahr, Mazandaran, Iran (batch number: 332992), then meticulously prepared for the extraction process. A voucher specimen (MAZ-A6-0101-001) was formally archived in the herbarium of Mazandaran University of Medical Sciences. The fermented biomass was carefully dried at 50 °C and subsequently ground using an electric grinder. The extraction process involved continuous maceration using 2 L of 70% ethanol solvent (hydroalcoholic). To initiate the extraction, an exact quantity of 200 g of dried and ground fermented biomass material was carefully positioned in a properly sized decanter funnel equipped with a cotton filter at the base. A 70% ethanol (hydroalcoholic) solvent was added to cover the fermented biomass completely, with an additional 3-cm layer above. The decanter was sealed and left undisturbed at room temperature for 48 h, following which the hydroalcoholic extract was allowed to drain by opening the valve.

Subsequent phases involved concentrating the extract using a rotary evaporator (Heidolph, Germany) under vacuum conditions, with the temperature maintained below 40 °C. The concentrated extracts were then subjected to freeze-drying (Zirbus, Germany) at temperatures of -45 °C to yield a powdered form. This powdered extract was carefully stored in glass containers within a refrigerator to preserve its integrity and quality for subsequent toxicological evaluations. The utilization of this preserved powdered material ensured the reliability of the toxicological tests conducted in this study (25).

Essential oil extraction and GC-MS analysis

Essential oils were extracted from 100 g of finely milled fermented biomass (particle size: 0.5-1 mm) using hydro-distillation with a Clevenger-type apparatus over 4 h. To enhance oil recovery, 3 mL of hexane was added. After extraction, the oils were dried using anhydrous sodium sulfate to eliminate residual moisture.

Gas chromatography-mass spectrometry (GC-MS) analysis (Agilent, USA) was performed on the oils using an HP-5ms capillary column (30 m × 0.25 mm i.d., 0.25 µm film thickness) and helium as the carrier gas. An injection volume of 1 µL was employed (split ratio of 10:1). The injector temperature was set at 250 °C. The oven temperature was programmed to rise from 60 °C to 220 °C at a rate of 5 °C per minute, with a final isothermal hold at 220 °C for 10 min. Compound identification was achieved by comparing retention indices with authentic standards or reference spectra from the W10N14.L and NIST14.L libraries (26,27).

Fig. S1. Samples of *Medusomyces gisevii* were obtained before the extraction process.

Measurement of DPPH radical-scavenging activity

The free radical scavenging efficacy of HEMG against stable diphenyl-1-picrylhydrazyl (DPPH) was assessed using spectrophotometric techniques employing the Blois method. The reduction in the absorption of the resultant solution signifies the compound's ability to scavenge free radicals. The characteristic dark purple color of DPPH in its stable state diminishes upon exposure to antioxidant agents.

To initiate the experiment, 1.5 mL of DPPH solution (0.15 mM) in methanol was mixed with different concentrations of HEMG and vitamin C as the standard compound. Following a 30-min incubation period in darkness at room temperature, the absorbance of the solutions was measured at 517 nm. The percentage inhibition of the DPPH radical was determined using the following equation:

$$Scavenging\ rate = \frac{A0 - AS}{A0} \times 100$$

where A0 represents the absorbance of the DPPH solution without the sample, and AS is the absorbance of the sample mixed with DPPH.

Finally, the EC_{50} value and the concentration of the sample required to scavenge 50% of the DPPH free radical were calculated based on the standard curve (28,29). All experimental procedures were conducted in triplicate to ensure the reliability and accuracy of the results.

Determination of total phenolic content

The total phenolic content (TPC) was measured using the Folin-Ciocalteu reagent with gallic acid as the standard reference in a spectrophotometric method with minor procedural adjustments. A solution was prepared by combining 25 mL of distilled water, 1 mL of the sample, 5 mL of Folin-Ciocalteu's reagent, and 4 mL of 6% Na_2CO_3. This mixture was incubated at room temperature for 60 min. Following the incubation period, the absorbance was measured at 765 nm, with a blank sample serving as the control reference.

The quantification of TPC was achieved through a standard curve established using gallic acid at concentrations of 6.25, 12.5, 25, 50, 100, and 200. The results were expressed as milligrams of gallic acid equivalents (GAE) per gram of dried extract (30).

Determination of total tannin content

Tannins were extracted from the sample, and the remaining phenolic compounds were quantified using the Folin-Ciocalteu method. The total phenolic content was compared in the presence and absence of tannins to determine the total tannin content (TTC), with polyvinylpolypyrrolidone (PVPP) employed as a tannin-binding agent.

Initially, 100 mg of PVPP was precisely weighed and deposited into a 100 × 12 mm test tube. Subsequently, 1.0 mL of distilled water and 1.0 mL of the tannin-rich extract were added to the tube. The solution was thoroughly mixed using vortexing and then placed in an incubator at 4 °C for 15 min. Following another round of vortexing, the tube underwent centrifugation at 3000 *g* for 10 min, separating a supernatant containing only simple phenolics from the tannins that had precipitated with the PVPP.

The phenolic content of the supernatant was determined using standard procedures, ensuring the extraction of at least double the volume (preferably triple) to accommodate the two-fold dilution of the extract and the expected loss of tannin-phenols due to their interaction with PVPP. Ultimately, the non-tannin phenolic content was reported based on the dry matter content (30).

Analysis of comprehensive ash content

The total ash content of the fermented biomass powder was determined by incinerating 10 g in a pre-weighed crucible at 600 °C for 6 h until a constant weight was achieved. Acid-insoluble ash was evaluated by treating the total ash with hydrochloric acid (HCl) and filtering through ashless paper. For sulfated ash quantification, 1 g of fermented biomass powder was mixed with 10 mL of sulfuric acid and heated at 600 °C for 30 min.

The water-soluble and water-insoluble ash fractions were determined by boiling the total ash in distilled water, filtering, and weighing the remaining residue. All tests were conducted thrice to ensure precision and reproducibility (27).

Animal studies

A total of 63 male albino mice, weighing 27 ± 2 g and aged between 8 and 10 weeks, were obtained from the Animal Research Institute at Mazandaran University of Medical Sciences in Sari, Iran. These mice were acclimatized for two weeks in standard conventional cages under controlled conditions of 25 ± 1 °C and a 12/12-h light/dark cycle, and were provided with unrestricted access to food and water. All experimental protocols were conducted in accordance with the guidelines approved by the Research Ethics Committee of Mazandaran University of Medical Sciences, Iran (IR.Mazums.4.Rec.1402.16124).

In the research, the mice were randomly divided into seven groups (9 per group) as follows: (1) ND: mice on a normal diet (ND) with free access to water; (2) HFD: mice on a high-fat diet (HFD, 58% fat) with a 10% w/v fructose solution as the drinking beverage; (3) VIT E: mice on a HFD supplemented with oral gavage of vitamin E at 20 mg/kg (BW/day); (4-7) HEMG: mice on a HFD supplemented with oral gavage of HEMG at 62.5, 125, 250, and 500 mg/kg BW/day. NAFLD was induced in the HFD groups during 12 weeks, as confirmed by biochemical and histological markers. After the establishment of the NAFLD, the administration of vitamin E and HEMG extracts *via* gavage lasted for 8 weeks, with the entire experimental period spanning 20 weeks. The dietary compositions utilized in this investigation are outlined in Table 1 (31,32). The duration and doses of HEMG used in a dose range were based on previous experimental studies that employed a similar dosage (33-35). The dosage of vitamin E used (20 mg/kg) was based on prior experimental studies that utilized a similar amount and demonstrated an antioxidant effect, reducing oxidative stress in mice with NAFLD (36-38).

Throughout the experimental duration, food consumption was monitored every two days, and body weight was recorded weekly. After 20 weeks, the mice were humanely euthanized using ketamine/xylazine (50 and 10 mg/kg, respectively; i.p) following a 12-h fast. Blood samples were collected *via* cardiac puncture immediately post-mortem, and serum was isolated by centrifugation at 3,500 rpm for 10 min at 4 °C, then stored at -80 °C for subsequent analysis. Tissues were promptly weighed and stored at -80 °C for further examination or preserved in 10% buffered formalin for histopathological assessments (1).

Analysis of serum enzyme markers

Levels of ALT, AST, ALP, TC, TG, LDL, and HDL were measured using assay kits and a fully automated biochemical analyzer (25,39).

Liver mitochondria isolation

Liver tissues were excised, washed with cold buffer at 4°C, minced, and homogenized. Mitochondria were isolated from the homogenate through differential centrifugation to explore mitochondrial oxidative stress markers. The isolated mitochondria were suspended in Tris buffer for evaluating mitochondrial function and oxidative damage, including measuring glutathione (GSH), lipid peroxidation (LPO), protein carbonyl (PC) levels, and the enzymatic activities of catalase (CAT) and SOD. ROS assessment was conducted by resuspending mitochondria in a respiration buffer (40).

Table 1. Dietary compositions used in this study.

Component	Normal diet (%)	High-fat diet (g)
Normal diet	-	150
Soy protein	-	500
Butter	-	810
Mineral mix	-	30
Vitamin mix	-	10
Crude protein	23	-
Salt	0.5	-
Calcium	1	-
Phosphorus	0.65	-
Tryptophan	0.25	-
Methionine	0.33	-
Lysine	1.15	-
Threonine	0.7	-
Crude fat	4	-
Crude fiber	4	-
Total weight (g)	1000	1500
Calories from fat (%)	15	58

Protein concentration measurement

The protein concentrations in each sample were assessed in the isolated heart mitochondria using the Bradford method, employing bovine serum albumin as the standard reference. In summary, samples were incubated with Coomassie blue, and after a 10-min incubation period, the absorbance was measured at 595 nm using a spectrophotometer (UV-1601 PC, Shimadzu, Japan) (40).

Mitochondrial function assessment (MTT assay)

An MTT evaluation protocol was utilized to assess mitochondrial viability. Samples containing 0.5 mg/mL of mitochondria were incubated with MTT (5 mg/mL solution in phosphate-buffered saline) for 30 min. The formazan produced by the mitochondria was subsequently quantified using an ELISA reader (BioTek, USA) at 570 nm (25,40).

Analysis of oxidative stress parameters

Determination of mitochondrial ROS

The ROS levels were assessed using the DCFH-DA reagent, which was prepared by dissolving 1.2 mg of DCFH-DA in 1 mL of ethanol. Initially, 10 µL of DCFH-DA was added to 1000 µL of the sample and incubated at 4 °C for 15 min. Following this incubation, a spectrofluorimeter (Jasco, Japan) was utilized to measure the absorbance at an excitation wavelength of 480 nm and an emission wavelength of 520 nm (40).

Measurement of mitochondrial PC

PC content was assessed *via* the DNPH assay. First, 100 µL of each sample was combined with 80 µL of 20% (w/v) trichloroacetic acid and incubated at 4 °C for 15 min. After centrifugation at 6,500 *g* for 10 min, the resulting pellet was resuspended in 500 µL of 0.1 M NaOH. Subsequently, 500 µL of 10 mM DNPH in 2 M HCl was added and incubated for 30 min. Absorbance was measured at 365 nm using an extinction coefficient of 22,000 M^{-1} cm^{-1} (40).

Measurement of mitochondrial LPO

Lipid peroxidation was evaluated by monitoring the formation of thiobarbituric acid reactive substances (TBARs), with malondialdehyde (MDA) concentration measured in µM as an indicator. To assess this, a 0.2 mL tissue homogenate was combined with 0.1 mL of TBA reagent, which consisted of 15% w/v TCA and 0.3% w/v TBA dissolved in 0.5 N HCl. After thorough mixing, the samples were boiled for 30 min and then cooled in an ice bath. Following this, 0.2 mL of n-butanol was added. The n-butanol layer was separated through centrifugation at 1,500 *g* for 10 min. Finally, the absorbance of the n-butanol layer was measured at 532 nm using an ELISA reader (BioTek, USA), and the quantity of TBARs was determined using a standard curve (40).

Measurement of mitochondrial GSH content

To determine the GSH content, 0.25 mL of 20% trichloroacetic acid was added to 1 mL of the mitochondrial fraction. After centrifugation at 1000 *g* for 20 min, 1 mL of the resulting clear supernatant was collected. To the supernatant, 2 mL of 0.3 M sodium hydrogen phosphate and 0.5 mL of 0.4% DTNB (prepared fresh on the same day, pH 7.2) were added to each sample, followed by a 15-min incubation. The absorbance was then measured at 412 nm, and the concentration of the sample was calculated and expressed in µM based on the standard curve of glutathione (30,40).

Antioxidant enzyme assay

To assess CAT activity, a test tube was combined with 20 µL of the mitochondrial fraction and with Tris buffer. Following this, 4800 µL of the reaction medium, consisting of sodium phosphate buffer (50 mM, pH 7.0) and H_2O_2 (10 mM), was added. The absorbance was measured at a wavelength of 240 nm. The activity of SOD was evaluated using an SOD assay kit according to the manufacturer's instructions (41,42).

Liver histopathology

Liver tissue specimens were fixed in 10% buffered formalin, subsequently embedded in paraffin, and sectioned to a thickness of 5 µm for hematoxylin and eosin (H&E) staining. Subsequently, an experienced pathologist examined the prepared slides under a light microscope to evaluate histopathological changes.

Statistical analysis

The results were presented as mean ± SD. Statistical analyses were conducted using

GraphPad Prism software, version 8. One-way analysis of variance (ANOVA) was performed, followed by the post-hoc Tukey test to compare the means. *P*-values < 0.05 were considered statistically significant.

RESULTS

GC-MS analysis of essential oil

The chemical composition of MG essential oil was evaluated using GC-MS. The total ion chromatogram (TIC) showed 40 distinct peaks identified during the 55-min run time (Fig. 1). Major compounds in the essential oil sample included cyclohexanol (7.93% of total peak area), carvacrol (6.52%), phenol (6.36%), cyclotetrasiloxane (5.27%), ethylene brassylate (4.96%), L-menthone (4.40%), and oxime-, methoxy-phenyl- (4.25%) (Table 2).

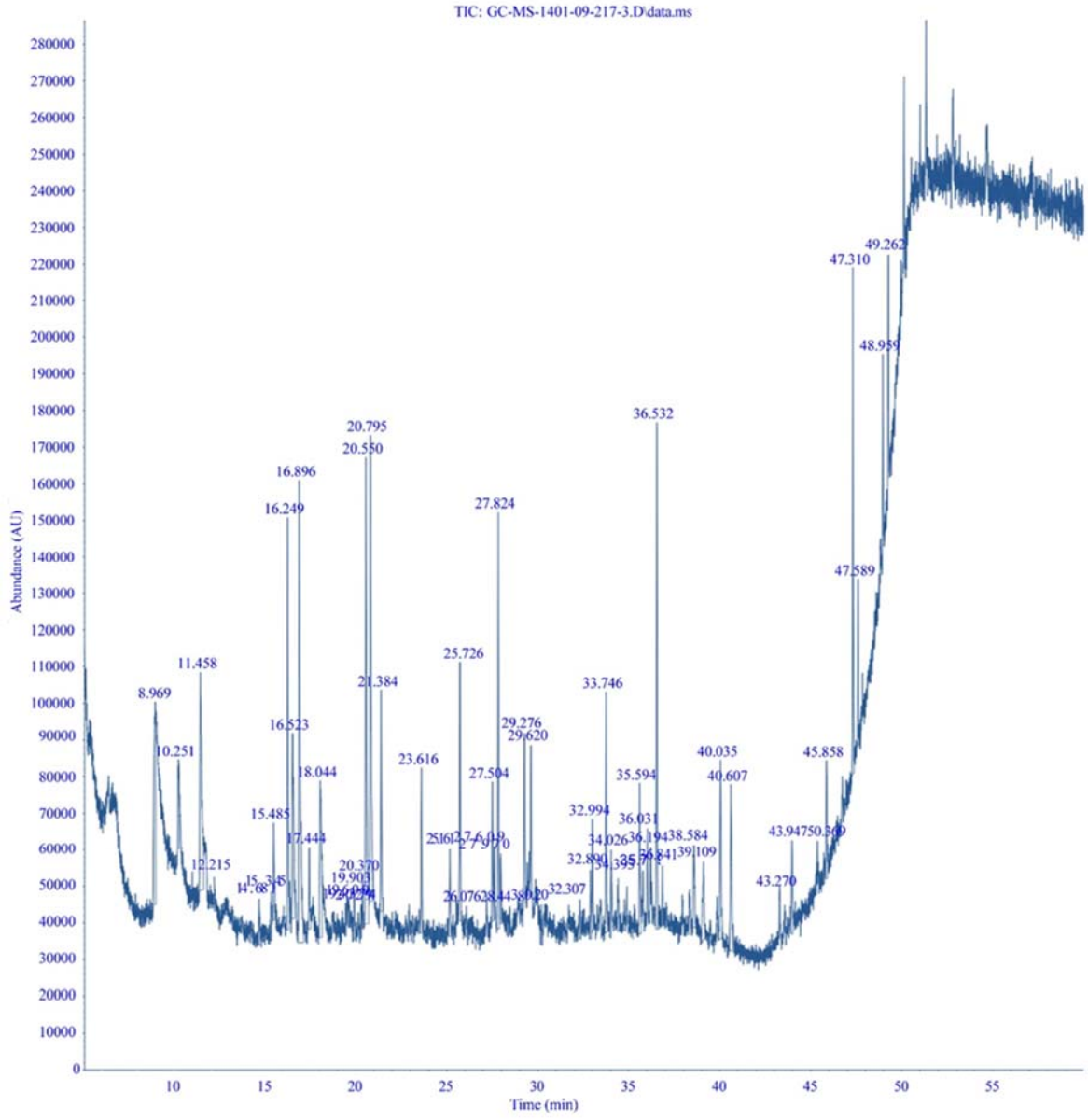

Fig. 1. Gas chromatography-mass spectrometry chromatogram of *Medusomyces gisevii* L. essential oil.

Table 2. Percentage composition of the gas chromatography-mass spectrometry chromatogram of *Medusomyces gisevii* L. essential oil.

Compound	RT (min)	RI	Area (%)
Oxime-, methoxy-phenyl-_	8.97	940	4.25
6,6-Dimethyl-4,8-dithiaundecan-1,11-Diol	10.25	974	1.23
Cyclotetrasiloxane, octamethyl-	11.46	1007	5.27
Adenosine	14.68	1103	0.52
5-hydroxy-8,8-dimethyl-4-phenylpyrano[2,3-h]chromen-2-one	15.35	1124	0.50
Methyl 5-amino-2-[(3-chlorophenyl)amino]-1,3-oxazole-4-carboxylate	15.49	1128	1.18
L-Menthone	16.25	1153	4.40
6-Aza-5,7,12,14-tetrathiapentacene	16.52	1162	3.15
Cyclohexanol, 5-methyl-2-(1-methylethyl)-	16.90	1174	7.93
3-Cyclohexene-1-methanol, alpha,alpha,4-trimethyl-, 1-acetate, (1r)-	17.44	1192	0.96
Dianhydromannitol	18.04	1206	3.35
8-Methyl-7-phenyl-2,4-di-n-piperidinoimidazo[1,2-f]purine	19.90	1240	0.59
Phenol, 2-methyl-5-(1-methylethyl)-	20.55	1252	6.36
Carvacrol	20.80	1257	6.52
Cyclohexasiloxane, dodecamethyl-	21.38	1267	2.32
Bicyclo[7.2.0]undec-4-ene, 4,11,11-trimethyl-8-methylene-,[1r-(1r*,4z,9s*)]-	23.62	1418	1.50
3,5-Dimethylamphetamine	25.16	1480	0.96
Cycloheptasiloxane, tetradecamet-	25.73	1501	2.55
MDMA methylene homolog	27.50	1540	1.37
5-APB	27.61	1543	0.60
(1ar,4s,4ar,7r,7as,7bs)-1,1,4,7-Tetramethyldecahydro-1h-cyclopropa[e]azulen-4-ol	27.82	1547	4.05
Pyrido[3,4-d]imidazole, 1,6-dicarboxylic acid	27.97	1551	0.82
Methyl 3-oxo-2-pentylcyclopentaneacetate	29.28	1579	1.76
Cyclooctasiloxane, hexadecamethyl-	29.62	1587	1.50
Cycloserine	32.89	1757	0.66
1,1,1,5,7,7,7-Heptamethyl-3,3-bis(trimethylsiloxy)tetrasiloxane	32.99	1759	1.10
1,2-Benzenedicarboxylic acid, bis(trimethylsilyl) ester	33.75	1775	2.49
2-Pyridinepropanoic acid	34.03	1781	0.78
Dibutyl phthalate	35.59	1963	1.72
Tetradecamethylcycloheptasiloxane	36.03	1986	0.90
Piperidinol	36.19	1994	0.73
Ethylene brassylate	36.53	2012	4.96
N-Desmethyltapentadol	36.84	2027	0.52
1-Octadecanamine, n-(1-methylethyl)-	38.58	2113	1.23
Satratoxin h	39.11	2134	1.53
Acetamide, 2-(hydroxyimino)-n-(4-methoxyphenyl)-	40.04	2170	2.60
Butyl citrate	40.61	2193	2.61
Carbamic acid, N-(cyanomethyl)-, ethyl ester	43.97	2320	1.30
trans-3,5-Dihydroxycyclopent-1-ene	45.86	2423	1.35
Di-(2-ethylhexyl)phthalate	47.31	2499	3.89

RT, Retention time; RI, retention indices on DB-5.

Antioxidant activity, TPC, and TTC

The DPPH free radical scavenging activity (IC_{50} value) of HEMG was determined and is detailed in Table 3. HEMG exhibited a DPPH free radical activity of 50.14 ± 3.56, while ascorbic acid (used as a standard) showed an IC_{50} value of 9.46 ± 2.21 µg/mL, indicating HEMG's strong free radical scavenging ability. Furthermore, HEMG's total phenolic and tannin content, expressed as mg of GAEs per g and mg per g of dried extract, varied based on the extraction solvent, as outlined in Table 3.

Determination of Ash content

Analysis of the MG sample revealed total ash content of 18.38%, with definite percentages for water-soluble ash (2.84%), water-insoluble ash (14.57%), acid-insoluble ash (5.73%), and sulfated ash (20.94%).

Effects of different doses of HEMG on serum biochemical parameters in NAFLD mice

The study demonstrated that serum ALT, AST, ALP, TC, TG, and LDL levels in serum were significantly altered in HFD-induced NAFLD mice compared to the ND groups. Treatment with HEMG (250 and 500 mg/kg) led to significant improvements in these parameters, while also positively affecting HDL levels (Figs. 2-8).

Table 3. Antioxidant activity, TPC, and TTC of HEMG. Data are expressed as means ± SD, n = 3.

Samples	DPPH (IC_{50}, µg/mL)	TPC (mg GAEs/g)	TTC (mg/g)
HEMG	50.14 ± 3.56	73.47 ± 0.85	62.56 ± 1.30
Ascorbic acid	9.46 ± 2.21	-	-

HEMG, Hydroalcoholic extract of *Medusomyces gisevii*; DPPH, 2,2-diphenyl-1-picrylhydrazyl; TPC, total phenolic content; GAE, gallic acid equivalent; TTC, total tannin content.

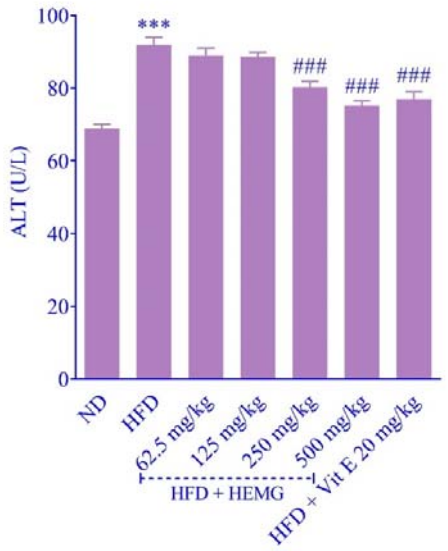

Fig. 2. Effect of different doses of HEMG administration on serum ALT levels. Data are presented as mean ± SD of 9 animals in each group. $^{***}P < 0.001$ indicates a significant difference in comparison with the ND group; $^{###}P < 0.001$ versus HFD-treated group. HEMG, *Medusomyces gisevii*; ALT, alanine transaminase; ND, normal diet; HFD, high-fat diet.

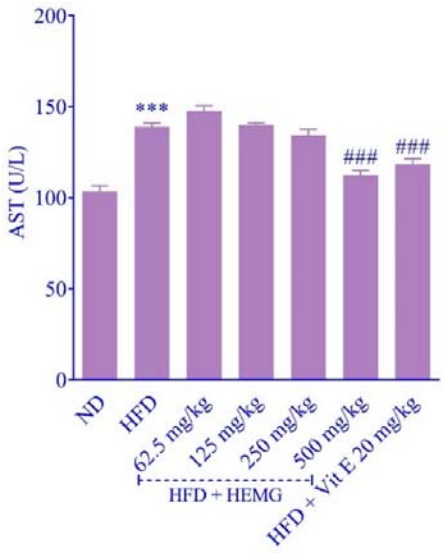

Fig. 3. Effect of different doses of HEMG administration on serum AST levels. Data are presented as mean ± SD of 9 animals in each group. $^{***}P < 0.001$ indicates a significant difference in comparison with the ND group; $^{###}P < 0.001$ versus the HFD-treated group. HEMG, *Medusomyces gisevii*; AST, aspartate aminotransferase; ND, normal diet; HFD, high-fat diet.

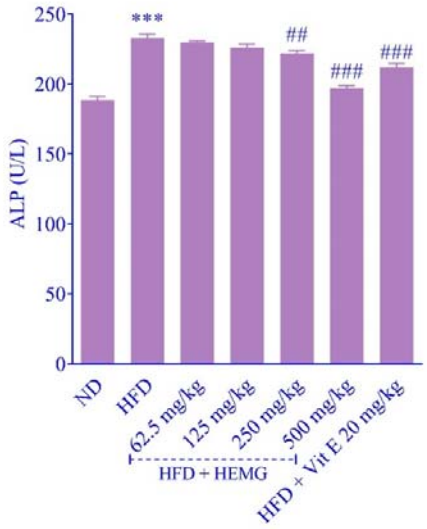

Fig. 4. Effect of different doses of HEMG administration on serum ALP levels. Data are presented as mean ± SD of 9 animals in each group. $^{***}P < 0.001$ indicates a significant difference in comparison with the ND group; $^{##}P < 0.01$ and $^{###}P < 0.001$ versus the HFD-treated group. HEMG, *Medusomyces gisevii*; ALP, alkaline phosphatase; ND, normal diet; HFD, high-fat diet.

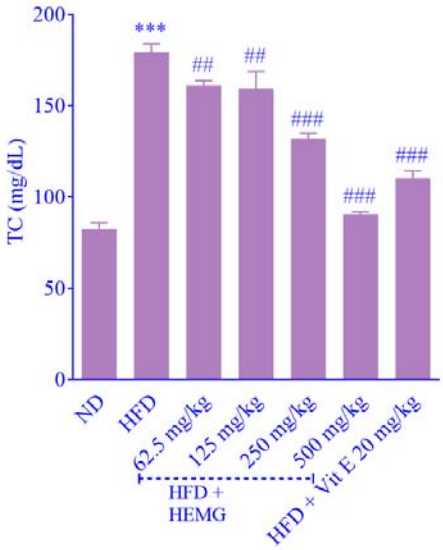

Fig. 5. Effect of different doses of HEMG administration on serum TC levels. Data are presented as mean ± SD of 9 animals in each group. $^{***}P < 0.001$ indicates a significant difference in comparison with the ND group; $^{##}P < 0.01$ and $^{###}P < 0.001$ versus the HFD-treated group. HEMG, *Medusomyces gisevii*; TC, total cholesterol; ND, normal diet; HFD, high-fat diet.

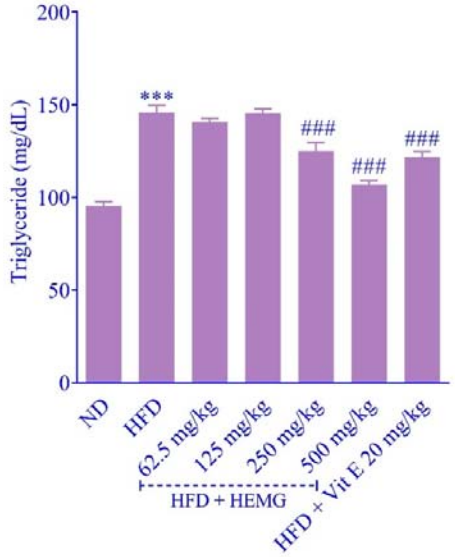

Fig. 6. Effect of different doses of HEMG administration on serum triglyceride levels. Data are presented as mean ± SD of 9 animals in each group. $^{***}P < 0.001$ indicates a significant difference in comparison with the ND group; $^{###}P < 0.001$ versus the HFD-treated group. HEMG, *Medusomyces gisevii*; ND, normal diet; HFD, high-fat diet.

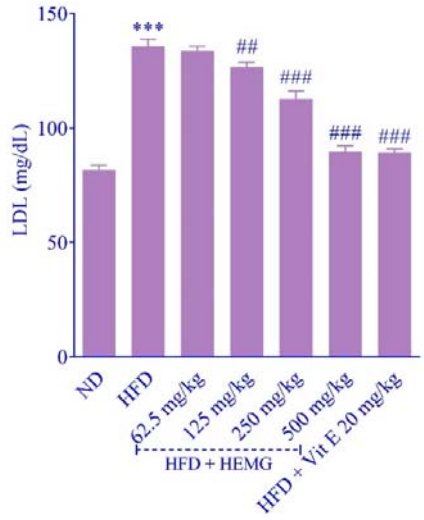

Fig. 7. Effect of different doses of HEMG administration on serum LDL levels. Data are presented as mean ± SD of 9 animals in each group. $^{***}P < 0.001$ indicates a significant difference in comparison with the ND group; $^{##}P < 0.01$ and $^{###}P < 0.001$ versus the HFD-treated group. HEMG, *Medusomyces gisevii*; LDL, low-density lipoproteins; ND, normal diet; HFD, high-fat diet.

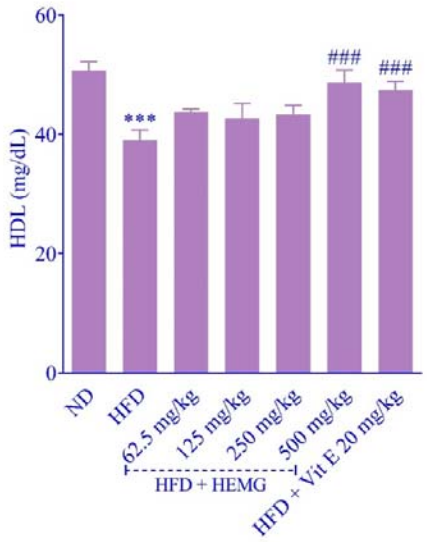

Fig. 8. Effect of different doses of HEMG administration on serum HDL levels. Data are presented as mean ± SD of 9 animals in each group. $^{***}P < 0.001$ indicates a significant difference in comparison with the ND group; $^{###}P < 0.001$ versus the HFD-treated group. HEMG, *Medusomyces gisevii*; LDL, high-density lipoproteins; ND, normal diet; HFD, high-fat diet.

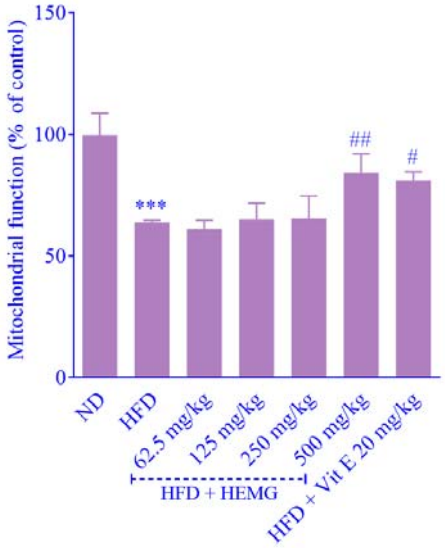

Fig. 9. Effect of different doses of HEMG administration on mitochondrial function in isolated mitochondria from mouse liver cells. Data are presented as mean ± SD of 9 animals in each group. $^{***}P < 0.001$ indicates a significant difference in comparison with the ND group; $^{#}P < 0.05$ and $^{##}P < 0.01$ versus the HFD-treated group. HEMG, *Medusomyces gisevii*; ND, normal diet; HFD, high-fat diet.

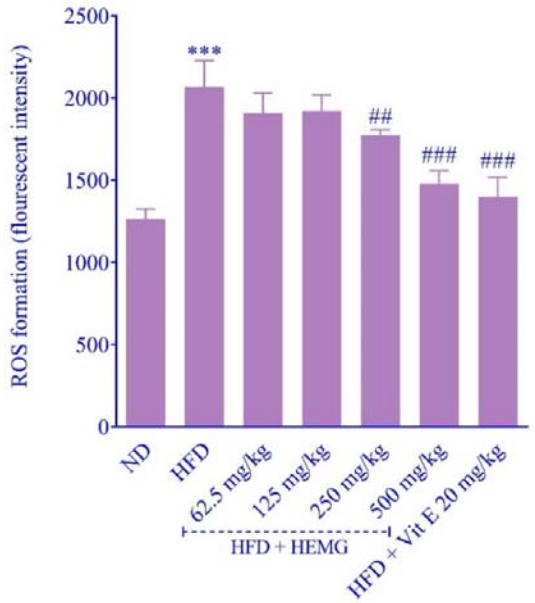

Fig. 10. Effect of different doses of HEMG administration on ROS formation in isolated mitochondria from mouse liver cells. Data are presented as mean ± SD of 9 animals in each group. $^{***}P < 0.001$ indicates a significant difference in comparison with the ND group; $^{##}P < 0.01$ and $^{###}P < 0.001$ versus the HFD-treated group. HEMG, *Medusomyces gisevii*; ND, normal diet; ROS, reactive oxygen species.

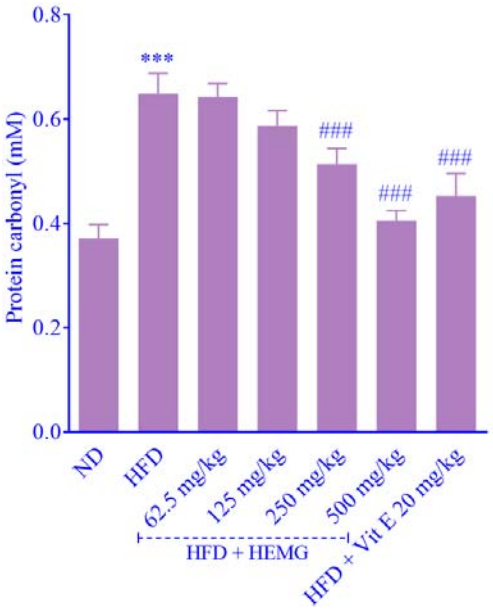

Fig. 11. Effect of different doses of HEMG administration on protein carbonyl level in isolated mitochondria from mouse liver cells. Data are presented as mean ± SD of 9 animals in each group. $^{***}P < 0.001$ indicates a significant difference in comparison with the ND group; $^{###}P < 0.001$ versus the HFD-treated group. HEMG, *Medusomyces gisevii*; ND, normal diet.

Effects of different doses of HEMG on oxidative stress parameters in NAFLD mice

The results of the current study indicated that mitochondrial function (MTT assay) was significantly reduced in the liver tissues of HFD-treated mice (63.80%) compared to the ND group. However, mitochondrial function significantly improved in the HEMG-treated group (500 mg/kg) to 84.33% when compared to the HFD-treated group (Fig. 9).

ROS levels were significantly elevated in HFD-treated mice compared to the normal diet group. HEMG treatment at 250 and 500 mg/kg significantly reduced ROS levels (Fig. 10).

PC levels were significantly elevated in HFD-treated mice compared to the ND group. However, a significant decrease in PC content was observed after HEMG treatment when compared with the HFD-treated group (Fig. 11).

The levels of MDA, as a lipid peroxidation product, were measured in this study. The results showed that the MDA levels significantly increased in HFD-treated mice compared to the ND group. Mitochondrial MDA levels significantly decreased in HEMG-treated groups at the doses of 62.5, 125, 250, and 500 mg/kg when compared with the HFD-treated group (Fig. 12).

GSH content was measured in the liver mitochondria, which was significantly reduced in HFD-treated mice compared to the ND group. Mitochondrial GSH content increased considerably in HEMG-treated groups at doses of 62.5, 125, 250, and 500 mg/kg when compared to the HFD-treated group (Fig. 13).

In this study, the CAT activity significantly decreased in HFD-treated mice when compared to the ND group. CAT activity in the mice liver mitochondria significantly increased by HEMG administration at the doses of 125, 250, and 500 mg/kg as compared to the HFD-treated group (Fig. 14).

The activity of the enzyme SOD was measured in the liver mitochondria of mice. A significant decrease in SOD activity was observed in the HFD-treated mice compared to the ND group. However, after administering HEMG (500 mg/kg), there was a significant increase in SOD activity compared to the HFD-treated group (Fig. 15).

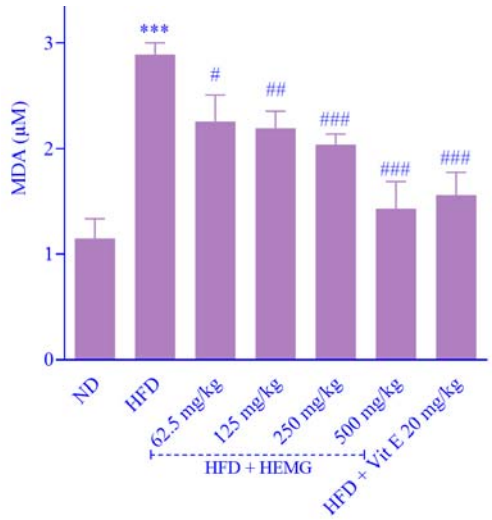

Fig. 12. Effect of different doses of HEMG administration on MDA level in isolated mitochondria from mouse liver cells. Data are presented as mean ± SD of 9 animals in each group. $^{***}P < 0.001$ indicates a significant difference in comparison with the ND group; $^{\#}P < 0.05$, $^{\#\#}P < 0.01$, $^{\#\#\#}P < 0.001$ versus the HFD-treated group. HEMG, *Medusomyces gisevii*; ND, normal diet; MDA, malondialdehyde.

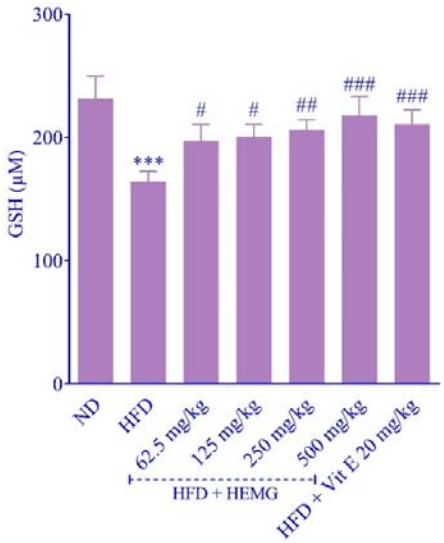

Fig. 13. Effect of different doses of HEMG administration on GSH level in isolated mitochondria from mouse liver cells. Data are presented as mean ± SD of 9 animals in each group. $^{***}P < 0.001$ indicates a significant difference in comparison with the ND group; $^{\#}P < 0.05$, $^{\#\#}P < 0.01$, $^{\#\#\#}P < 0.001$ versus the HFD-treated group. HEMG, *Medusomyces gisevii*; ND, normal diet; GSH, glutathione.

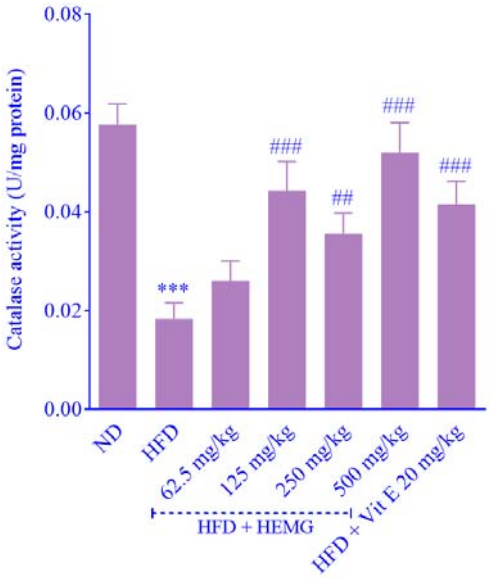

Fig. 14. Effect of different doses of HEMG administration on CAT level in isolated mitochondria from mouse liver cells. Data are presented as mean ± SD of 9 animals in each group. $^{***}P < 0.001$ indicates a significant difference in comparison with the ND group; $^{\#\#}P < 0.01$ and $^{\#\#\#}P < 0.001$ versus the HFD-treated group. HEMG, *Medusomyces gisevii*; ND, normal diet; CAT, catalase.

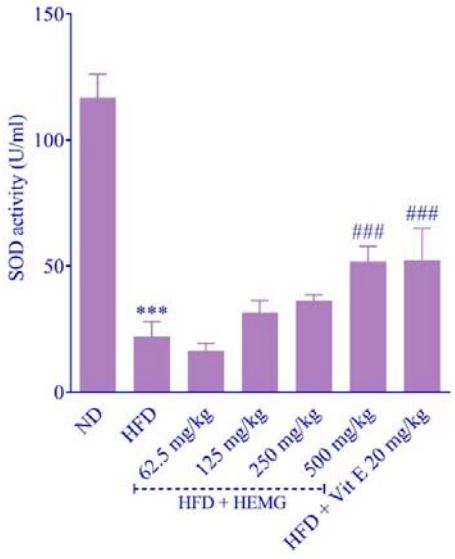

Fig. 15. Effect of different doses of HEMG administration on SOD level in isolated mitochondria from mouse liver cells. Data are presented as mean ± SD of 9 animals in each group. $^{***}P < 0.001$ indicates a significant difference in comparison with the ND group; $^{\#\#\#}P < 0.001$ versus the HFD-treated group. HEMG, *Medusomyces gisevii*; ND, normal diet; SOD, superoxide dismutase.

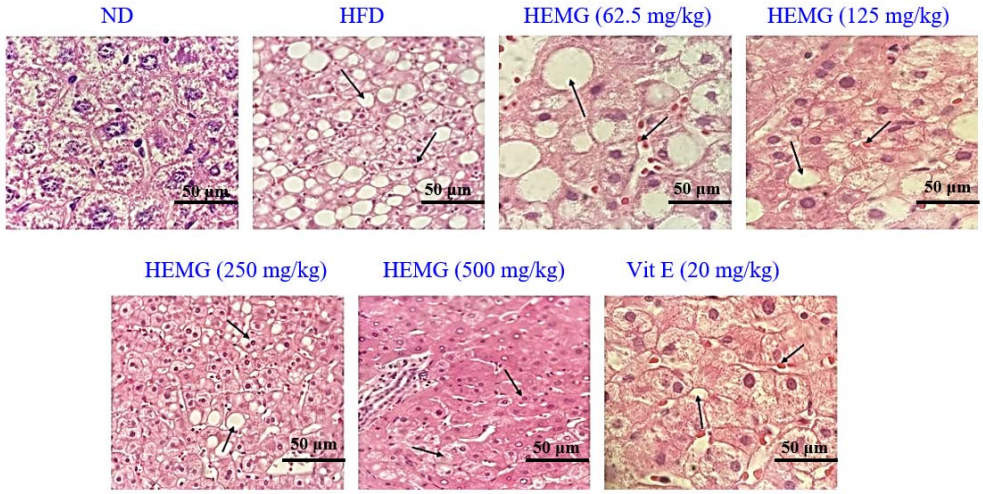

Fig. 16. Effect of different doses of HEMG administration on liver histopathological changes in the liver tissue of mice (magnification ×400). The liver sections of mice fed an ND or HFD were stained with hematoxylin and eosin (H&E; scale bars: 50 µm). HEMG, *Medusomyces gisevii*; ND, normal diet; HFD, high-fat diet.

Effects of different doses of HEMG on histopathological changes in liver tissue

Histopathological examination revealed that HFD-induced NAFLD mice exhibited fatty liver development characterized by increased lipid droplets. Treatment with HEMG, particularly at 500 mg/kg/BW/day, significantly reduced hepatic lipid droplets and improved liver conditions, mitigating hepatic steatosis (Fig. 16 and Table 4). These results underscore the potential of HEMG treatment in ameliorating hepatic steatosis in NAFLD mice.

Table 4. Grading of hepatic steatosis in NAFLD mice after administration of different doses of HEMG.

Histopathological Finding	ND	HFD	HEMG (62.5 mg/kg)	HEMG (125 mg/kg)	HEMG (250 mg/kg)	HEMG (500 mg/kg)	Vit E (20 mg/kg)
Steatosis	0	+++	++	++	+	0 (Nearly normal liver tissue)	0 (Less than 5% steatosis)

+, Mild steatosis (grade 1); ++, moderate steatosis (grade 2); +++, severe steatosis (grade 3); HEMG, hydroalcoholic extract of *Medusomyces gisevii*; ND, normal diet; HFD, high fat diet.

DISCUSSION

NAFLD stands as a prevalent liver disorder and a significant consequence of obesity and metabolic syndrome. Our research establishes the efficacy of administering a HEMG in reducing liver fat accumulation and addressing various liver histopathological issues, notably steatosis induced by an HFD.

While ongoing investigations into the effects of MG extract on NAFLD are progressing, existing studies emphasize the potent anti-obesity properties of extracts (43,44). The relationship between improvements in biochemical factors and hepatic steatosis observed in histopathological examinations is relative. Typically, biochemical factors show improvement first, while histopathological damage, such as steatosis and inflammation, improves more gradually over time. It is important to emphasize that fatty liver disease is reversible, but it can recur if there is a lack of physical activity and weight gain. This study demonstrates that HEMG intervention effectively normalized abnormal serum levels of ALT, AST, ALP, TG, TC, LDL, and HDL in HFD-exposed mice. Moreover, evaluations of liver pathology indicated a significant reduction in hepatic lipid droplet presence following HEMG treatment. Previous animal studies have suggested beneficial effects of Kombucha tea on serum factors and histopathological liver damage (34,35,45). Several studies have identified the chemical constituents of Kombucha from diverse regions (46,47). Employing GC/MS technology, for the first time, we categorized 40 odor-active compounds of MG into eight groups, including alcohols, ketones, alkenes, esters, alkanes, aromatics, acids, and ethers. In this study, we identified cyclohexanol, 5-methyl-2-(1-methylethyl)-, as a prominent compound in MG essential oil. Notably, polyphenols and other phytochemical compounds have been linked to the antioxidant effects of HEMG (48-50). The antioxidant analysis results from the DPPH assay highlighted HEMG's substantial antioxidant capacity, although lower than that of vitamin C. Furthermore, our assessment of TPC and TTC of HEMG revealed elevated levels of total phenolics and tannins, consistent with prior investigations across diverse experimental models (50-52). Thus far, no studies have examined the potential toxicity, side effects, or long-term safety of HEMG. These important issues require further investigation.

The role of oxidative stress in NAFLD complications has been well-documented in laboratory models (53,54). This study unveiled a notable reduction in mitochondrial function in the NAFLD group compared to controls, with a marked enhancement in mitochondrial function observed following HEMG administration, particularly at the highest dose. Previous research has indicated that lipid accumulation in hepatocytes triggers mitochondrial dysfunction, leading to increased oxidative stress levels (55,56).

It is known that HFD-induced tissue damage due to oxidative stress can occur through increased ROS generation and direct depletion of antioxidant reserves (57,58). Mitochondrial dysfunction can precipitate oxidative stress, creating a cycle characterized by elevated mitochondrial ROS and subsequent organelle dysregulation (30). In the context of this study, we hypothesized that HEMG significantly mitigates ROS formation. Notably, Mun *et al.* demonstrated a significant reduction in ROS formation in mice co-supplemented with a water extract of *Curcuma longa* L. and an HFD (1).

PC serves as a reliable marker for assessing oxidative stress conditions, with its implications in NAFLD development and progression warranting further investigation. Recent insights suggest that protein carbonylation may behave as a thiol-mediated signaling mechanism, with thioredoxin activity playing a crucial role in reducing protein carbonylation levels (59,60).

The present study aligns with established research by demonstrating increased protein carbonylation in the NAFLD group, meaningfully alleviated post-HEMG administration.

MDA, a recognized indicator of oxidative stress, reflects excessive lipid peroxidation (61). Studies have demonstrated that oxidative damage stems from excessive production of lipid peroxidation molecules, protein oxidation products, and diminished activity of antioxidant enzymes (62). Elevated MDA levels can lead to oxidative damage to cell membranes, proteins, nucleic acids, and other biomolecules by binding with them, with hepatic MDA levels reflecting hepatocyte lipid peroxidation extent (63). Our research demonstrated higher liver MDA levels in HFD mice compared to ND mice, with a significant reduction following HEMG administration, indicating a reduction in oxidative stress.

Given the liver's significance in detoxification and oxidation processes, susceptibility to oxidative stress is heightened *in vivo*. Oxidative stress arises from an imbalance between oxidative and antioxidant actions, often due to increased free radical generation and diminished antioxidant activity (64). This study revealed a substantial decrease in liver GSH content in the model group compared to controls, indicating heightened oxidative stress induced by HFD in mice. Since GSH content is responsible for the decomposition of ROS, the reduction in GSH content may make the liver tissue of the examined mice more susceptible to oxidative stress (65). The antioxidant levels serve as critical indicators of cytotoxic damage in liver tissue. HEMG functions as an antioxidant, helping to neutralize free radicals, enhancing antioxidant enzyme activities such as SOD and GSH, while reducing MDA levels, a lipid peroxide, in NAFLD mouse livers. In our investigation, HEMG treatment, particularly at the highest dose, increased damage *via* antioxidant properties.

Liver function alterations can exacerbate oxidative stress effects, compromising antioxidant defense system enzymes due to elevated reactive species associated with NAFLD, thereby compromising non-enzymatic and enzymatic antioxidant defenses (66). CAT and SOD play crucial roles in combating free radicals, offering insights into oxidative stress levels. CAT functions in peroxidase detoxification by converting toxic peroxides into non-toxic compounds, protecting cells from peroxidase-induced damage. Meanwhile, SOD, an antioxidant metalloenzyme, catalyzes superoxide anion radicals' conversion into oxygen (O_2) and hydrogen peroxide (H_2O_2) (67). This study confirmed alterations in antioxidant defense, with HEMG inclusion restoring CAT and SOD activities, thereby enhancing redox balance and ameliorating impaired antioxidant defenses in liver tissues. Moreover, HEMG enhanced impaired antioxidant defense systems in mice, demonstrated by CAT, SOD, and GSH in liver tissues. These findings suggest HEMG may possess hepatoprotective properties, mitigating damage resulting from oxidative stress.

CONCLUSION

The research focuses on the therapeutic potential of an HEMG for managing NAFLD, a common condition associated with obesity and metabolic syndrome. The study demonstrates HEMG's effectiveness in reducing liver fat accumulation, addressing liver histopathological issues such as steatosis induced by an HFD, and its antioxidant properties, chemical composition, and impact on oxidative stress parameters in NAFLD mice.

Key findings highlight HEMG's ability to normalize serum enzyme levels, enhance antioxidant enzyme activities, reduce lipid peroxidation levels, mitigate oxidative stress in liver tissues, impact mitochondrial function, protein carbonylation, and GSH levels. The reduction in ROS formation and restoration of antioxidant defenses by HEMG suggest its potential in ameliorating HFD-induced liver damage and improving overall liver function.

The results underscore the importance of further research on HEMG and its components in NAFLD treatment. Future studies could explore molecular mechanisms, optimal dosage, and potential therapeutic applications in clinical settings. By showcasing HEMG's therapeutic advantages, the study proposes valuable insights for effective NAFLD treatments and innovative interventions in combating this complex liver disorder.

Acknowledgments

The authors are grateful to Mazandaran University of Medical Sciences for their financial support through the Grant No. 16124.

Conflict of interest statement

The authors declared no conflicts of interest in this study.

Authors' contributions

R. Zare Gashti performed the experiments and wrote the original draft. M. Shokrzadeh conceived and designed the study. M. Shokrzadeh and M. Karami supervised the study. R. Zare Gashti, S. Parsay, M. Karami, and M. Modanloo reviewed and edited the manuscript. R. Zare Gashti, M. Karami, S. Parsay, E. Habibi, A. Abbasi, and H. Asadi Khalili analyzed and interpreted the data; contributed reagents, materials, analysis tools, or data. All authors have read and approved the finalized article. Each author has fulfilled the authorship criteria and affirmed that this article represents honest and original work.

Data availability statement

The data used to support the findings of this study are available from the corresponding author upon reasonable request.

AI declaration

During the preparation of this work, the author(s) used Grammarly to improve readability and language. After using this tool, the author(s) reviewed and edited the content and take full responsibility for the content of the publication.

REFERENCES

1. Mun J, Kim S, Yoon HG, You Y, Kim OK, Choi KC, *et al*. Water extract of *Curcuma longa L*. ameliorates non-alcoholic fatty liver disease. Nutrients. 2019;11(10):2536,1-13. DOI: 10.3390/nu11102536.
2. Guo X, Yin X, Liu Z, Wang J. Non-alcoholic fatty liver disease (NAFLD) pathogenesis and natural products for prevention and treatment. Int J Mol Sci. 2022;23(24):15489,1-18. DOI: 10.3390/ijms232415489.
3. Chalasani N, Younossi Z, Lavine JE, Diehl AM, Brunt EM, Cusi K, *et al*. The diagnosis and management of non-alcoholic fatty liver disease: practice guideline by the American Association for the Study of Liver Diseases, American College of Gastroenterology, and the American Gastroenterological Association. Hepatology. 2012;55(6):2005-2023. DOI: 10.1002/hep.25762.
4. Ye Q, Zou B, Yeo YH, Li J, Huang DQ, Wu Y, *et al*. Global prevalence, incidence, and outcomes of non-obese or lean non-alcoholic fatty liver disease: a systematic review and meta-analysis. Lancet Gastroenterol Hepatol. 2020;5(8):739-752. DOI: 10.1016/S2468-1253(20)30077-7.
5. Milić S, Lulić D, Štimac D. Non-alcoholic fatty liver disease and obesity: biochemical, metabolic and clinical presentations. World J Gastroenterol. 2014;20(28):9330-9337. DOI: 10.3748/wjg.v20.i28.9330.
6. Feng G, Li XP, Niu CY, Liu ML, Yan QQ, Fan LP, *et al*. Bioinformatics analysis reveals novel core genes associated with nonalcoholic fatty liver disease and nonalcoholic steatohepatitis. Gene. 2020;742:144549,1-5. DOI: 10.1016/j.gene.2020.144549.
7. Malekinejad H, Zeynali-Moghaddam S, Rezaei-Golmisheh A, Alenabi A, Malekinejad F, Alizadeh A, *et al*. Lupeol attenuated the NAFLD and PCOS-induced metabolic, oxidative, hormonal, histopathological, and molecular injuries in mice. Res Pharm Sci. 2023;18(5):551-565. DOI: 10.4103/1735-5362.383710.
8. Heeren J, Scheja L. Metabolic-associated fatty liver disease and lipoprotein metabolism. Mol Metab. 2021;50:101238,1-17. DOI: 10.1016/j.molmet.2021.101238.
9. Morales D, Miguel M, Garcés-Rimón M. Pseudocereals:a novel source of biologically active peptides. Crit Rev Food Sci Nutr. 2021;61(9):1537-1544. DOI: 10.1080/10408398.2020.1761774.
10. Gonzalez A, Huerta-Salgado C, Orozco-Aguilar J, Aguirre F, Tacchi F, Simon F, *et al*. Role of oxidative stress in hepatic and extrahepatic dysfunctions during nonalcoholic fatty liver disease (NAFLD). Oxid Med Cell Longev. 2020;2020:1617805,1-16. DOI: 10.1155/2020/1617805.
11. Presa N, Clugston RD, Lingrell S, Kelly SE, Merrill Jr AH, Jana S, *et al*. Vitamin E alleviates non-alcoholic fatty liver disease in phosphatidylethanolamine N-methyltransferase deficient mice. Biochim Biophys Acta, Mol Basis Dis. 2019;1865(1):14-25. DOI: 10.1016/j.bbadis.2018.10.010.
12. Songtrai S, Pratchayasakul W, Arunsak B, Chunchai T, Kongkaew A, Chattipakorn N, *et al*. Cyclosorus terminans extract ameliorates insulin resistance and non-alcoholic fatty liver disease (NAFLD) in high-fat diet (HFD)-induced obese rats. Nutrients. 2022;14(22):4895,1-19. DOI: 10.3390/nu14224895.
13. Sumida Y, Yoneda M, Seko Y, Takahashi H, Hara N, Fujii H, *et al*. Role of vitamin E in the treatment of non-alcoholic steatohepatitis. Free Radic Biol Med. 2021;177:391-403. DOI: 10.1016/j.freeradbiomed.2021.10.017.

14. Li S, Duan F, Li S, Lu B. Administration of silymarin in NAFLD/NASH: a systematic review and meta-analysis. Ann Hepatol. 2024;29(2):101174,1-12. DOI: 10.1016/j.aohep.2023.101174.
15. Noureddin M, Mato JM, Lu SC. Nonalcoholic fatty liver disease: update on pathogenesis, diagnosis, treatment and the role of S-adenosylmethionine. Exp Biol Med. 2015;240(6):809-820. DOI: 10.1177/1535370215579161.
16. Xiao L, Xiong H, Deng Z, Peng X, Cheng K, Zhang H, *et al*. Tetrastigma hemsleyanum leaf extracts ameliorate NAFLD in mice with low-grade colitis *via* the gut-liver axis. Food Funct. 2023;14(1):500-515. DOI: 10.1039/D2FO03028D.
17. Xu J, Jia W, Zhang G, Liu L, Wang L, Wu D, *et al*. Extract of *Silphium perfoliatum L.* improve lipid accumulation in NAFLD mice by regulating AMPK/FXR signaling pathway. J Ethnopharmacol. 2024;327:118054. DOI: 10.1016/j.jep.2024.118054.
18. Jiang G, Ramachandraiah K, Murtaza MA, Wang L, Li S, Ameer K. Synergistic effects of black ginseng and aged garlic extracts for the amelioration of nonalcoholic fatty liver disease (NAFLD) in mice. Food Sci Nutr. 2021;9(6):3091-3099. DOI: 10.1002/fsn3.2267.
19. Le TNH, Choi HJ, Jun HS. Ethanol extract of liriope platyphylla root attenuates non-alcoholic fatty liver disease in high-fat diet-induced obese mice *via* regulation of lipogenesis and lipid uptake. Nutrients. 2021;13(10):3338,1-13. DOI: 10.3390/nu13103338.
20. Bondareva NI, Timchenko LD, Dobrynya YM, Alieva EVe, Rzhepakovsky IV, Sizonenko M, *et al*. Influence of biologically active substances from Kombucha (*Medusomyces gisevii*) on rat gut microbiota with experimental antibiotic-associated dysbiosis. Indian J Anim Sci. 2017;87(5):624-629. DOI: 10.56093/ijans.v87i5.70256.
21. Flyurik EA, Ermakova OS. *Medusomyces gisevii*: cultivation, composition, and application. 2022;11(1):152-161. DOI: 10.21603/2308-4057-2023-1-563.
22. Martínez Leal J, Valenzuela Suárez L, Jayabalan R, Huerta Oros J, Escalante-Aburto A. A review on health benefits of kombucha nutritional compounds and metabolites. CyTA-J Food. 2018;16(1):390-399. DOI: 10.1080/19476337.2017.1410499.
23. Watawana MI, Jayawardena N, Gunawardhana CB, Waisundara VY. Health, wellness, and safety aspects of the consumption of kombucha. J Chem. 2015;2015(1):591869,1-11. DOI: 10.1155/2015/591869.
24. Abshenas J, Derakhshanfar A, Ferdosi MH, Hasanzadeh S. Protective effect of kombucha tea against acetaminophen-induced hepatotoxicity in mice: a biochemical and histopathological study. Comp Clin Path. 2012;21(6):1243-1248. DOI: 10.1007/s00580-011-1273-9.
25. Dashti A, Shokrzadeh M, Karami M, Habibi E. Phytochemical identification, acute and subchronic oral toxicity assessments of hydroalcoholic extract of *Acroptilon repens* in BALB/c mice: a toxicological and mechanistic study. Heliyon. 2022;8(2):1-12. DOI: 10.1016/j.heliyon.2022.e08940.
26. Enayatifard R, Akbari J, Babaei A, Rostamkalaei SS, Hashemi SMH, Habibi E. Anti-microbial potential of nano-emulsion form of essential oil obtained from aerial parts of *Origanum vulgare L.* as food additive. Adv Pharm Bull. 2020;11(2):327,1-8. DOI: 10.34172/apb.2021.028.
27. Habibi E, Hemmati P, Arabnozari H, Khalili HA, Sharifianjazi F, Enderami SE, *et al*. Phytochemical analysis and immune-modulatory potential of *Trichaptum biforme* polysaccharides: implications for cancer. Int J Biol Macromol. 2024;280:135691. DOI: 10.1016/j.ijbiomac.2024.135691.
28. Balogun FO, Ashafa AOT. Cytotoxic, kinetics of inhibition of carbohydrate-hydrolysing enzymes and oxidative stress mitigation by flavonoids roots extract of Dicoma anomala (Sond.). Asian Pac J Trop Med. 2018;11(1):24-31. DOI: 10.4103/1995-7645.223530.
29. Wanyo P, So-In C. The protective effect of Thai rice bran on N-acetyl-ρ-aminophen-induced hepatotoxicity in mice. Res Pharm Sci. 2024;19(2):188-202. DOI: 10.4103/RPS.RPS_210_23.
30. Arabnozari H, Shaki F, Saberi Najjar A, Sharifianjazi F, Sarker SD, Habibi E, *et al*. The effect of *Polygonum hyrcanicum Rech. f.* hydroalcoholic extract on oxidative stress and nephropathy in alloxan-induced diabetic mice. Sci Rep. 2024;14(1):18117,1-11. DOI: 10.1038/s41598-024-69220-x.
31. Wilson CG, Tran JL, Erion DM, Vera NB, Febbraio M, Weiss EJ. Hepatocyte-specific disruption of CD36 attenuates fatty liver and improves insulin sensitivity in HFD-fed mice. Endocrinology. 2016;157(2):570-585. DOI: 10.1210/en.2015-1866.
32. Velázquez AM, Bentanachs R, Sala-Vila A, Lázaro I, Rodríguez-Morató J, Sánchez RM, *et al*. ChREBP-driven DNL and PNPLA3 expression induced by liquid fructose are essential in the production of fatty liver and hypertriglyceridemia in a high-fat diet-fed rat model. Mol Nutr Food Res. 2022;66(7):2101115,1-11. DOI: 10.1002/mnfr.202101115.
33. Shariatzadeh SMA, Miri SA, Cheraghi E. The protective effect of Kombucha against silver nanoparticle-induced toxicity on testicular tissue in NMRI mice. Andrologia. 2021;53(3):e13982,1-10. DOI: 10.1111/and.13982.
34. Alaei Z, Doudi M, Setorki M. The protective role of Kombucha extract on the normal intestinal microflora, high-cholesterol diet caused hypercholesterolemia, and histological structure changes in New Zealand white rabbits. Avicenna J Phytomed. 2020;10(6):604-614. PMCID: PMC7711297.
35. Hyun J, Lee Y, Wang S, Kim J, Kim J, Cha J, *et al*. Kombucha tea prevents obese mice from developing hepatic steatosis and liver damage. Food Sci Biotechnol. 2016;25(3):861-866. DOI: 10.1007/s10068-016-0142-3.

36. Karimian G, Kirschbaum M, Veldhuis ZJ, Bomfati F, Porte RJ, Lisman T. Vitamin E attenuates the progression of non-alcoholic fatty liver disease caused by partial hepatectomy in mice. PLoS One. 2015;10(11):e0143121,1-12. DOI: 10.1371/journal.pone.0143121.
37. Ni Y, Nagashimada M, Zhuge F, Zhan L, Nagata N, Tsutsui A, *et al*. Astaxanthin prevents and reverses diet-induced insulin resistance and steatohepatitis in mice: a comparison with vitamin E. Sci Rep. 2015;5(1):17192,1-15. DOI: 10.1038/srep17192.
38. He W, Xu Y, Ren X, Xiang D, Lei K, Zhang C, *et al*. Vitamin E ameliorates lipid metabolism in mice with nonalcoholic fatty liver disease via Nrf2/CES1 signaling pathway. Dig Dis Sci. 2019;64(11):3182-3191. DOI: 10.1007/s10620-019-05657-9.
39. Liang M, Huo M, Guo Y, Zhang Y, Xiao X, Xv J, *et al*. Aqueous extract of *Artemisia capillaris* improves non-alcoholic fatty liver and obesity in mice induced by high-fat diet. Front Pharmacol. 2022;13:1084435,1-16. DOI: 10.3389/fphar.2022.1084435.
40. Zare Gashti R, Mohammadi H. Sodium dithionate ($Na_2S_2O_4$) induces oxidative damage in mice mitochondria heart tissue. Toxicol Rep. 2022;9: 1391-1397. DOI: 10.1016/j.toxrep.2022.06.016.
41. Fathi H, Ebrahimzadeh MA, Ziar A, Mohammadi H. Oxidative damage induced by retching; antiemetic and neuroprotective role of *Sambucus ebulus L*. Cell Biol Toxicol. 2015;31(4-5):231-239. DOI: 10.1007/s10565-015-9307-8.
42. Akbari G, Abasi MR, Gharaghani M, Nouripoor S, Shakerinasab N, Azizi M, *et al*. Antioxidant and hepatoprotective activities of *Juniperus excelsa M. Bieb* against bile duct ligation-induced cholestasis. Res Pharm Sci. 2024;19(2):217-227. DOI: 10.4103/RPS.RPS_52_23.
43. Ou X, Chen J, Li B, Yang Y, Liu X, Xu Z, *et al*. Multiomics reveals the ameliorating effect and underlying mechanism of aqueous extracts of *Polygonatum sibiricum* rhizome on obesity and liver fat accumulation in high-fat diet-fed mice. Phytomedicine. 2024;132:155843,1-18. DOI: 10.1016/j.phymed.2024.155843.
44. Luo X, Zhang B, Pan Y, Gu J, Tan R, Gong P. *Phyllanthus emblica* aqueous extract retards hepatic steatosis and fibrosis in NAFLD mice in association with the reshaping of intestinal microecology. Front Pharmacol. 2022;13:893561,1-19. DOI: 10.3389/fphar.2022.893561.
45. Lee C, Kim J, Wang S, Sung S, Kim N, Lee HH, *et al*. Hepatoprotective effect of kombucha tea in rodent model of nonalcoholic fatty liver disease/nonalcoholic steatohepatitis. Int J Mol Sci. 2019;20(9):2369,1-18. DOI: 10.3390/ijms20092369.
46. Majumder S, Ghosh A, Chakraborty S, Bhattacharya M. Withdrawal of stimulants from tea infusion by SCOBY during kombucha fermentation: a biochemical investigation. Int J Food Ferment Tech. 2020;10(1):21-26. DOI: 2277-9396.01.2020.5.
47. Wang Z, Ahmad W, Zhu A, Geng W, Kang W, Ouyang Q, *et al*. Identification of volatile compounds and metabolic pathway during ultrasound-assisted kombucha fermentation by HS-SPME-GC/MS combined with metabolomic analysis. Ultrason Sonochem. 2023;94:106339,1-16. DOI: 10.1016/j.ultsonch.2023.106339.
48. Cardoso RR, Neto RO, dos Santos D'Almeida CT, do Nascimento TP, Pressete CG, Azevedo L, *et al*. Kombuchas from green and black teas have different phenolic profile, which impacts their antioxidant capacities, antibacterial and antiproliferative activities. Food Res Int. J. 2020;128:108782,1-10. DOI: 10.1016/j.foodres.2019.108782.
49. Jakubczyk K, Kałduńska J, Kochman J, Janda K. Chemical profile and antioxidant activity of the kombucha beverage derived from white, green, black and red tea. Antioxidants. 2020;9(5):447,1-15. DOI: 10.3390/antiox9050447.
50. La Torre C, Fazio A, Caputo P, Plastina P, Caroleo MC, Cannataro R, *et al*. Effects of long-term storage on radical scavenging properties and phenolic content of kombucha from black tea. Molecules. 2021;26(18):5474,1-14. DOI: 10.3390/molecules26185474.
51. Oliveira JT, da Costa FM, da Silva TG, Simões GD, dos Santos Pereira E, da Costa PQ, *et al*. Green tea and kombucha characterization: phenolic composition, antioxidant capacity and enzymatic inhibition potential. Food Chem. 2023;408:135206,1-7. DOI: 10.1016/j.foodchem.2022.135206.
52. Zhou DD, Saimaiti A, Luo M, Huang SY, Xiong RG, Shang A, *et al*. Fermentation with tea residues enhances antioxidant activities and polyphenol contents in kombucha beverages. Antioxidants. 2022;11(1):155,1-17. DOI: 10.3390/antiox11010155.
53. Lou D, Fang Q, He Y, Ma R, Wang X, Li H, *et al*. Oxymatrine alleviates high-fat diet/streptozotocin-induced non-alcoholic fatty liver disease in C57BL/6 J mice by modulating oxidative stress, inflammation and fibrosis. Biomed Pharmacother. 2024;174:116491,1-10. DOI: 10.1016/j.biopha.2024.116491.
54. Yang Z, Zhang L, Liu J, Chan ASC, Li D. Saponins of tomato extract improve non-alcoholic fatty liver disease by regulating oxidative stress and lipid homeostasis. Antioxidants (Basel). 2023;12(10):1848,1-16. DOI: 10.3390/antiox12101848.
55. Engin AB, Engin A. Obesity and lipotoxicity. Springer; 2017. pp. 443. DOI: 10.1007/978-3-319-48382-5.
56. Li Z, Berk M, McIntyre TM, Gores GJ, Feldstein AE. The lysosomal-mitochondrial axis in free fatty acid-induced hepatic lipotoxicity. Hepatology. 2008;47(5):1495-1503. DOI: 10.1002/hep.22183.

57. Yu D, Chen G, Pan M, Zhang J, He W, Liu Y, *et al*. High-fat diet-induced oxidative stress blocks hepatocyte nuclear factor 4α and leads to hepatic steatosis in mice. J Cell Physiol. 2018;233(6): 4770-4782.
DOI: 10.1002/jcp.26270.
58. Cole BK, Feaver RE, Wamhoff BR, Dash A. Non-alcoholic fatty liver disease (NAFLD) models in drug discovery. Expert Opin Drug Discov. 2018;13(2):193-205.
DOI: 10.1080/17460441.2018.1410135.
59. Wong CM, Marcocci L, Liu L, Suzuki YJ. Cell signaling by protein carbonylation and decarbonylation. Antioxid Redox Signal. 2010;12(3):393-404.
DOI: 10.1089/ars.2009.2805.
60. Wong CM, Zhang Y, Huang Y. Bone morphogenic protein-4-induced oxidant signaling via protein carbonylation for endothelial dysfunction. Free Radic Biol Med. 2014;75:178-190.
DOI: 10.1016/j.freeradbiomed.2014.07.035.
61. Weismann D, Hartvigsen K, Lauer N, Bennett KL, Scholl HP, Issa PC, *et al*. Complement factor H binds malondialdehyde epitopes and protects from oxidative stress. Nature. 2011;478(7367):76-81.
DOI: 10.1038/nature10449.
62. Kowalska M, Piekut T, Prendecki M, Sodel A, Kozubski W, Dorszewska J. Mitochondrial and nuclear DNA oxidative damage in physiological and pathological aging. DNA Cell Biol. 2020;39(8):1410-1420.
DOI: 10.1089/dna.2019.5347.
63. Martín-Fernández M, Arroyo V, Carnicero C, Sigüenza R, Busta R, Mora N, *et al*. Role of oxidative stress and lipid peroxidation in the pathophysiology of NAFLD. Antioxidants. 2022;11(11):2217,1-10.
DOI: 10.3390/antiox11112217.
64. Luo H, Chiang HH, Louw M, Susanto A, Chen D. Nutrient sensing and the oxidative stress response. Trends Endocrinol Metab. 2017;28(6):449-460.
DOI: 10.1016/j.tem.2017.02.008.
65. Meng Y, Liu Y, Fang N, Guo Y. Hepatoprotective effects of *Cassia semen* ethanol extract on non-alcoholic fatty liver disease in experimental rat. Pharm Biol. 2019;57(1):98-104.
DOI: 10.1080/13880209.2019.1568509.
66. de Freitas Carvalho MM, Lage NN, de Souza Paulino AH, Pereira RR, de Almeida LT, da Silva TF, *et al*. Effects of açai on oxidative stress, ER stress, and inflammation-related parameters in mice with high-fat diet-fed induced NAFLD. Sci Rep. 2019;9(1):8107,1-11.
DOI: 10.1038/s41598-019-44563-y.
67. Gündüz AM, Demir H, Toprak N, Akdeniz H, Demir C, Arslan A, *et al*. The effect of computed tomography on oxidative stress level and some antioxidant parameters. Acta Radiol. 2021;62(2): 260-265.
DOI: 10.1177/0284185120922135.